

Rapid Detection of Chlorothalonil Fungicide Using Anisotropic Gold Nanoparticles Plasmonic Sensor

Nur Liyana Razali^{a,b}, Marlia Morsin^{a,b,*}, Rahmat Sanudin^{a,b}, Nur Zehan An'nisa Md Shah^c, and Suratun Nafisah^d

^aMicroelectronics & Nanotechnology – Shamsuddin Research Centre (MiNT-SRC), Institute for Integrated Engineering, Universiti Tun Hussein Onn Malaysia, 86400, Parit Raja, Batu Pahat, Johor, Malaysia

^bDepartment of Electronics Engineering, Faculty of Electrical and Electronic Engineering, Universiti Tun Hussein Onn Malaysia, 86400, Parit Raja, Batu Pahat, Johor, Malaysia

^cSunlight Electrical Pte Ltd, Chin Bee Road, 618679, Jurong, Singapore

^dDepartment of Electrical Engineering, Institut Teknologi Sumatera (ITERA), Lampung Selatan, 35365, Indonesia

*Corresponding author. Tel.: +607-453-8612; e-mail: marlia@uthm.edu.my

Received 17 July 2025, Revised 25 August 2025, Accepted 27 October 2025

ABSTRACT

Anisotropic gold nanoparticles (AuNPs) are well-known for their remarkable optical properties, particularly their dual-band surface plasmon resonance (SPR) behaviour. In this study, we harnessed these unique features to develop a rapid fungicide detection system. The sensing approach relies on monitoring changes in the intensity and position of the SPR peaks, with the absorbance spectrum serving as the primary detection signal. Upon light exposure, the sensor could detect chlorothalonil in at least three seconds. Notably, chlorothalonil alone does not produce significant SPR peaks; however, when combined with AuNPs, two distinct SPR bands emerge, corresponding to the transverse (t-SPR) and longitudinal (l-SPR) resonance modes. As chlorothalonil concentration increases, the absorbance intensity of the AuNPs also rises, likely due to an increase in refractive index around the nanoparticles. Stability assessments revealed minimal variation in SPR peak values, which were consistently recorded at 1.30 ± 0.00001 and 1.18 ± 0.00001 a.u. over a 600-second period. In repeatability tests, the sensor demonstrated dependable performance across six measurement cycles, with the signal reliably returning to baseline after each medium change. The AuNPs exhibited a fast optical response, reaching maximum spectral shifts within 30 seconds. These findings underscore the potential of anisotropic AuNPs as an effective platform for rapid, consistent, and sensitive detection of fungicides.

Keywords: Gold Nanoparticles thin film, Localized Surface Plasmon Resonance, Plasmonic Sensor, Seed-Mediated Growth Method

1. INTRODUCTION

Modern agriculture depends heavily on pesticides to safeguard crops from pests and diseases, which can otherwise cause substantial yield losses [1], [2]. Among these, fungicides play a particularly vital role in preventing fungal infections that threaten crop health and productivity [3]. However, the overuse or improper handling of fungicides can lead to serious environmental consequences and pose health risks to humans [4]. The presence of pesticide residues in food and the environment has become a growing public health concern, primarily due to their potential toxicity and the risks associated with prolonged exposure [2].

Among the commonly used fungicides, chlorothalonil stands out for its widespread application in agriculture. It is routinely applied to various crops, including potatoes, tomatoes, peanuts, and green onions, due to its broad-spectrum antifungal properties [5], [6], [7]. Despite its effectiveness, chlorothalonil has raised significant safety concerns. The United States Environmental Protection Agency (EPA) has classified it as a probable human carcinogen [8], and long-term exposure has been linked to serious health issues such as kidney and stomach tumors,

according to evaluations by the Food and Agriculture Organization of the United Nations and the World Health Organization (FAO/WHO) Expert Committee. These risks underscore the need to develop fast, reliable, and sensitive detection techniques to monitor chlorothalonil residues in food products and environmental samples.

Several analytical techniques have been implemented for pesticide detection to address this need. Traditional methods, including gas chromatography (GC) [9] and high-performance liquid chromatography (HPLC) [10], are known for their high sensitivity and accuracy. However, their application often requires elaborate sample preparation, expensive equipment, and extended analysis times. As a result, attention has increasingly shifted toward alternative approaches such as biosensors. Among these, sensors based on localized surface plasmon resonance (LSPR) have gained prominence for offering a simpler, faster, and more cost-effective solution, without compromising sensitivity or selectivity [11], [12], [13].

LSPR sensors leverage the unique optical properties of noble metal nanoparticles, such as gold and silver, to detect chemical and biological analytes. The resonance condition of these nanoparticles is highly dependent on their shape,

size, and the surrounding medium, making them ideal candidates for sensing applications [14], [15], [16]. Among the various nanostructures used in LSPR sensing, anisotropic gold nanoparticles (AuNPs) exhibit enhanced plasmonic responses due to their dual-band surface plasmon resonance (SPR) peaks. These properties allow for improved sensitivity and selectivity in chemical detection.

In previous studies, different anisotropic AuNP structures, such as nanorods, nanoplates, and nanobipyramids [14], [17], [18], have been synthesized for various sensing applications. However, most of these nanostructures are produced in solution form, leading to stability issues and limitations in practical applications. To overcome these challenges, this study focuses on developing anisotropic

AuNPs in a thin-film form using the seed-mediated growth method (SMGM). This approach enhances the stability and reusability of the sensing material, making it more suitable for real-world applications.

This study aims to fabricate and characterize an LSPR-based plasmonic sensor using anisotropic AuNP thin films for the rapid detection of chlorothalonil (Figure 1). The sensor's performance is evaluated based on its sensitivity, stability, and repeatability in different test environments. By utilizing the optical properties of AuNPs, this work provides a promising platform for efficient pesticide monitoring, contributing to improved food safety and environmental protection.

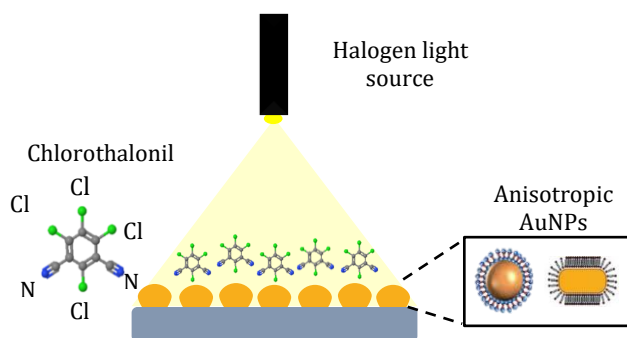


Figure 1. Schematic diagram of plasmonic sensor structure.

2. MATERIALS AND METHODS

2.1. Materials

Six chemical reagents were precisely weighed using a high-accuracy analytical balance and subsequently diluted with deionized (DI) water, exhibiting a resistivity of approximately 18.2 M Ω ·cm, supplied by a Pure Lab UHQ ELGA system. Each reagent was prepared according to its required molarity for the experimental procedures. The materials used included Hydrogen Tetrachloroaurate (HAuCl₄·3H₂O, 99.9% purity), trisodium citrate dihydrate, polyvinylpyrrolidone (PVP, average molecular weight 55,000), and sodium borohydride (NaBH₄, 98% purity), all sourced from Sigma Aldrich, USA. Additionally, hexadecyltrimethylammonium bromide (CTAB, \geq 98% purity) and ascorbic acid (AA) were obtained from Sigma Aldrich, China. Another batch of PVP with the same molecular weight (55,000) was procured from Emory Chemicals.

2.2. Preparation of AuNPs Thin Film as a Sensing Material

AuNPs thin films were fabricated using a modified two-step SMGM [19]. The first step is the seeding process, and the second is the AuNPs growth process.

Firstly, the AuNPs seeding was performed by immersing the ITO substrate in 2 ml Na₃C₆H₅O₇, 0.5 ml NaBH₄, 18 ml DI water, and 0.5 ml HAuCl₄·3H₂O for 2 hours at room

temperature. The formation of gold nanoseeds was indicated by the change in the color of the solution from light yellow to reddish-orange. Then, the samples were removed from the seeding solution, gently washed with DI water, and dried.

To strengthen the gold nanoseeds on the surface, the AuNPs thin films were annealed at 150 °C for 1 hour under vacuum. The growth of AuNPs was monitored to observe their density and shape. Initially, 10 ml of PVP was mixed with 8 ml of CTAB and later 2 ml of DI water containing 0.1 ml of AA and 0.5 ml of HAuCl₄·3H₂O was added to the mixture. The solution was shaken vigorously to mix the reagents for around 10 seconds. Its color changes from light yellow to colorless after the mixing process. The solution was then left to age undisturbed at 28 °C.

2.3. Characterization of AuNPs

The physical, morphological and optical properties of the AuNPs were investigated. Firstly, the physical characterization was done by observing the color variations of the solution through the seeding and growth process. Next, the morphological properties of the samples were verified using a field emission scanning electron microscope (FESEM, JEOL JSM-7600F, Japan). The accelerating voltage used was 5 kV, and the magnification was \times 50000. The optical absorbance was measured from 300 to 1000 nm using a UV/Visible scanning spectrophotometer (Shimadzu UV-1800, Japan).

2.4. Setup for Plasmonic Sensor System

The chlorothalonil was detected using the optimized AuNPs thin film as a sensing material by a plasmonic sensor system. The sensing response was recorded according to the absorbance spectrum. Figure 2 shows the setup of the plasmonic sensor using AuNPs as the active sensing material. The sensing system consists of a duplex fiber optic, a spectrometer, a light source, a sensor chamber, and a computer.

Figure 3 shows the sensing mechanism of the plasmonic sensor. The sensor operating mode was set to absorption spectroscopy with reflectance mode. A halogen light source is used to induce plasmon resonance of the AuNPs. The operating mode allows light reflected from the AuNPs thin film to be collected by the fiber optics probe and sent to the spectrometer to be analyzed. A signal corresponding to chlorothalonil's presence can be obtained based on the

resonance peak position and intensity change. The light absorption data were then analyzed using OceanView software.

To ensure the stable operation of the sensor, the system was allowed to warm up for at least 10 minutes. Next, the LSPR spectrum of the AuNPs thin film in air and 1 ml DI water was recorded and used as a blank reference. Then, the LSPR spectrum of the AuNPs thin film was recorded again in a 1 ml solution containing chlorothalonil. The spectrum responses were recorded for 600 seconds. All measurements were carried out in triplicate.

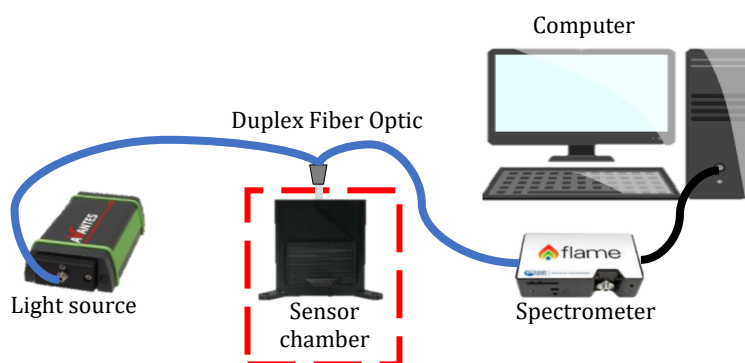


Figure 2. Sensor setup for LSPR-based chlorothalonil. AuNPs thin film is used as a sensing material.

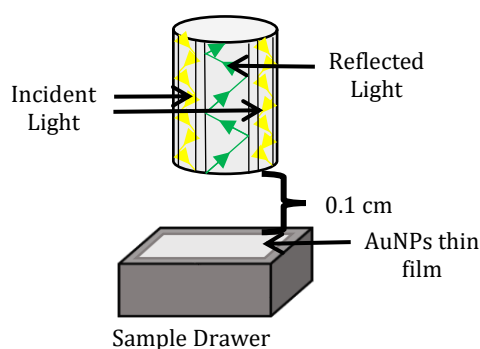


Figure 3. Sensing mechanism of the plasmonic sensor.

2.5. Sensor Operation

The spectrometer was connected to the computer via USB, and the light source was turned on. Within the OceanView software, the "Absorbance only" mode was chosen. The sample solution was positioned at the centre of the sensor chamber's drawer for detecting chlorothalonil fungicide. The analyte consisted of chlorothalonil dissolved in liquid, while AuNPs were the sensing element. The performance of AuNPs in terms of sensitivity, stability, and repeatability toward chlorothalonil was evaluated in three different environments: air, DI water, and chlorothalonil solution.

After powering on, the sensor system required 30 minutes to reach a stable operating condition. Subsequently, the integration time and peak, set near 80% of the maximum signal, were calibrated by placing deionized water in the drawer as a reference. Since the sample was a liquid, this calibration step was essential to remove any absorption effects caused by the reference solution before conducting the actual measurements. The sensor transmits light from the source through an optical fibre, which then passes into the solution. Specific wavelengths of light are reflected back through the fibre, captured by the spectrometer, and the resulting data—comprising wavelength and intensity—is sent to the computer for analysis.

2.6. Preparation of Chlorothalonil

The chlorothalonil fungicide is a fine, light beige powder and contains 50% of the active ingredient chlorothalonil. The trade name of this fungicide in the industry is Etanil WP, Manufacturer. A stock solution of chlorothalonil was prepared by diluting the powder with DI water and stored at room temperature. Twelve different molarities of chlorothalonil were prepared: 1.0, 2.0, 3.0, 4.0, 5.0, 10.0, 15.0, 20.0, 25.0, 30.0, 35.0 and 40.0 mM. For each 1.0 mM of chlorothalonil stock solution, 5 ml of DI water was mixed with 1.33 mg of chlorothalonil powder and shaken for 30 seconds at room temperature. The procedure was repeated for the other eleven molarity concentrations of chlorothalonil.

3. RESULTS AND DISCUSSION

3.1. Properties of AuNPs Thin Film

AuNPs were successfully synthesized and coated as a thin film on the quartz substrate using wet chemical synthesis known as SMGM. Figure 4(a) shows the optical response and morphological image of a comparison sample, gold nanosphericals (AuNSs). The reddish solution was the final color of AuNSs after the growth process, and the optical response of AuNSs showed only one t-SPR resonance peak at 545 nm. Anisotropic AuNPs, such as rods, triangles, spheres, and other irregular shapes, are grown on the substrate surface, as shown in Figure 4(b). In this study, the by-products were called spherical and irregular shapes. The violet AuNPs expressed two resonance peaks at 550 and 651 nm. The two bands of surface plasmon resonance are t-SPR and l-SPR, which correspond to the width and length of nanoparticles, respectively. Therefore, AuNPs have an extra sensing parameter compared to AuNSs, owing to the longitudinal SPR band that enhances the detection of chlorothalonil.

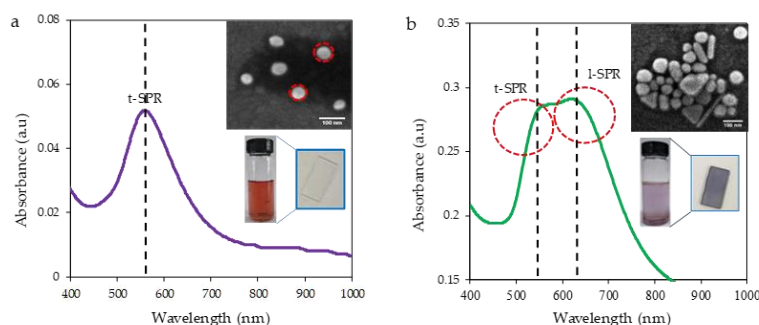


Figure 4. Optical properties of (a) AuNSs and (b) Anisotropic AuNPs. Insets are FESEM images at 50,000 magnifications with a scale bar of 100 nm.

3.2. Sensitivity Test of AuNPs Thin Film Towards Different Analytes

The plasmonic sensor's sensitivity was examined across four distinct media: A – air (containing only pure AuNPs), B – a 30.0 mM chlorothalonil solution without AuNPs, C – AuNPs dispersed in deionized water, and D – AuNPs combined with a 30.0 mM chlorothalonil solution. The corresponding spectral changes in the AuNPs' behavior across these environments are illustrated in Figure 5. The absorption peaks' position and intensity, specifically for the t-SPR and l-SPR bands, were analyzed. As depicted, samples incorporating AuNPs consistently demonstrated two prominent absorption peaks, corresponding to t-SPR and l-SPR. Conversely, the chlorothalonil solution without nanoparticles exhibited no notable peaks in these regions, highlighting the importance of AuNPs in enhancing detection capability. The plasmonic effect of AuNPs is influenced by their morphology, composition, and surrounding dielectric environment. These effects stem from the oscillation of free electrons at the nanoparticle surface when exposed to incident light [20].

According to Mie theory, the refractive index (η) of the medium surrounding gold nanoparticles plays a crucial role in determining their surface plasmon resonance (SPR) wavelength [21]. For instance, when the nanoparticles are suspended in air ($\eta = 1.00$), the resonance peak is observed at 860.16 nm. Introducing water ($\eta = 1.33$) causes a red shift of 49.54 nm, shifting the peak to 909.70 nm. A similar, and slightly more pronounced, red shift occurs when DI water is replaced with a chlorothalonil solution, which has a higher refractive index ($\eta = 1.633$). This consistent trend demonstrates that increasing the refractive index of the surrounding medium leads to a red shift in the plasmon resonance peak, making it a useful parameter for detecting analytes such as chlorothalonil.

These spectral shifts arise from local refractive index changes due to the adsorption or desorption of molecules on the nanoparticle surfaces, affecting the SPR wavelength. Additionally, the absorbance intensity also varies depending on the surrounding medium. Gold nanoparticles typically show higher peak intensities in air than in liquid media, a result of the lower refractive index of air.

The findings outlined in Table 1 reinforce the optical behaviour observed in the plasmonic response of gold nanoparticles. In an air medium, the t-SPR peak of the AuNPs is recorded at 450.46 nm with an absorbance intensity of 0.50 a.u. When these nanoparticles are introduced into DI water, the t-SPR peak shifts to 399.36 nm, a response attributable to the increased refractive index of the surrounding medium. Exposure to a chlorothalonil solution leads to a further shift of the t-SPR peak to 463.99 nm, signalling a significant interaction between the nanoparticles and the chlorothalonil molecules. A similar trend is observed in the l-SPR mode: the initial peak at 860.16 nm in air shifts to 909.70 nm in DI water, and then to 907.84 nm in the presence of chlorothalonil, with a corresponding absorbance increase to 0.47 a.u. These spectral shifts provide strong evidence of

the sensor's sensitivity to variations in the surrounding refractive index.

It is also worth emphasizing that chlorothalonil alone does not generate any notable absorbance peaks, underscoring the pivotal role of AuNPs in enabling detection. The consistent shifts in both t-SPR and l-SPR modes upon exposure to chlorothalonil highlight a robust interaction between the analyte and the nanoparticle surface, confirming the reliability of the detection mechanism. The rise in absorbance observed with increasing chlorothalonil concentration further demonstrates the practical effectiveness of this plasmonic sensor system for monitoring pesticide residues.

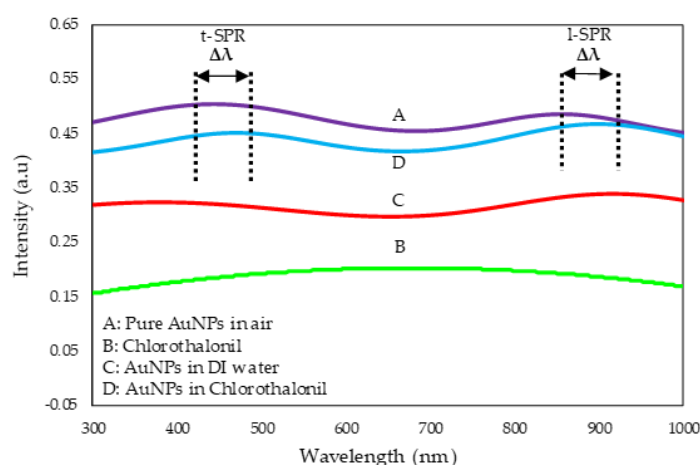


Figure 5. Optical response spectra of (A) Pure AuNPs in air medium, (B) Pure chlorothalonil, AuNPs in (C) deionized water, and (D) 30.0 mM chlorothalonil.

Table 1 Peak positions of t-SPR and l-SPR bands for AuNPs in three different media

Medium	t-SPR		l-SPR	
	Wavelength (nm)	Absorbance (a.u.)	Wavelength (nm)	Absorbance (a.u.)
Pure AuNPs (Air)	450.46	0.50	860.16	0.48
Chlorothalonil	-	0.20	-	0.20
AuNPs + DI water	399.36	0.34	909.70	0.34
AuNPs + Chlorothalonil	463.99	0.45	907.84	0.47

3.3. Stability and Repeatability Test of AuNPs Thin Film

The stability of AuNPs was tested for 10 minutes (600 seconds) by observing the absorbance intensity peaks for both l-SPR and t-SPR responses. In the presence of light, the sensor can detect the targeted analyte within 3 seconds. Plasmon resonance peak appears at 1.30 ± 0.00001 a.u and 1.18 ± 0.00001 a.u, referring to t-SPR and l-SPR, respectively. However, the peak intensity change was insignificant for both l-SPR and t-SPR peaks. Besides, the longitudinal and transverse peaks showed a linear correlation trend, stable for at least 600 seconds. Thus, this observation indicates that AuNPs thin film can be used as an active sensing material to detect chlorothalonil by exploiting surface plasmonic resonance phenomena.

A repeatability test was done to validate the repeatability potential of the plasmonic sensor for chlorothalonil detection. The LSPR peak position of DI water was used as a reference, whereas the LSPR peak position of chlorothalonil was measured as the test analyte. Two peak wavelengths of t-SPR and l-SPR were observed, and AuNPs showed exceptional sensitivity to chlorothalonil. Figure 6 shows the responses of AuNPs in the presence of 30.0-mM chlorothalonil within 60-second time intervals. Reproducibility of the sensor's optical response was assessed through multiple exposure cycles in alternating media. Each transition between analyte and reference yielded consistent recovery of absorbance peaks, underscoring the robustness and reliability of the thin film

under repeated use [22]. The repeatability tests for DI water and chlorothalonil solution mediums were carried out with resonance peak positions at 450 nm for t-SPR and 860 nm for l-SPR, repeated for six cycles for both peaks. Figure 6 shows the repeatability test on the absorbance intensity of AuNPs in air and 30 mM chlorothalonil. Meanwhile, Figure 7 shows the repeatability test on the absorbance intensity of AuNPs in air and DI water. The optical responses of AuNPs were measured, with an average absorbance intensity of 1.25 ± 0.0166 a.u. for l-SPR, whereas t-SPR showed absorbance with an intensity of 1.19 ± 0.0083 a.u. The spectrum difference between water and chlorothalonil solution mediums was 0.22%. In addition, the optical

response of the AuNPs was fast, with a typical response time (time to reach maximal change) of 30 s. When the chlorothalonil solution was changed to water to recover the original condition, the recovery period took about 30 seconds. These results demonstrate the optical properties of AuNPs that can be used for the sensitive detection of chlorothalonil, corresponding to the change of the surrounding medium. The repeatability test was repeated four times on different samples to observe its trends. Hence, the AuNPs have a good ability as a sensing material in a chlorothalonil sensor based on their fast response and recovery times of the LSPR resonance peaks in each medium.

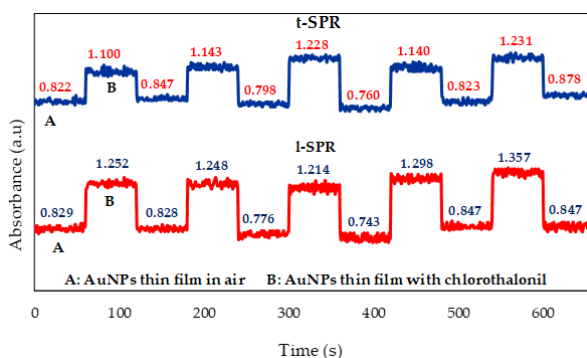


Figure 6. Repeatability test of the absorbance intensity of AuNPs: A) AuNPs thin film exposed to air, and B) AuNPs thin film exposed to 30 mM chlorothalonil.

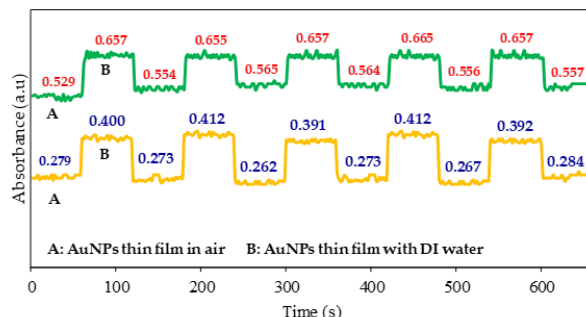


Figure 7. Repeatability test of the absorbance intensity of AuNPs: A) AuNPs thin film in air, and B) AuNPs thin film in DI water.

3.4. Sensitivity Test of LSPR-based Sensor Towards Different Concentrations of Chlorothalonil

The sensing sensitivity of the AuNPs-based LSPR sensor for chlorothalonil detection was analyzed using its peak absorbance intensity (ΔI) and wavelength shift ($\Delta \lambda$) [23]. The chlorothalonil solutions were diluted with 5 mL of deionized water for twelve concentrations of 1.0, 2.0, 3.0, 4.0, 5.0, 10.0, 15.0, 20.0, 25.0, 30.0, 35.0, and 40.0 mM. Figure 8 shows the optical response of the chlorothalonil solution for different concentrations. From the optical responses of t-SPR and l-SPR, the absorbance intensity of AuNPs was proportional to the chlorothalonil concentrations of the fungicide due to increased index bias. The second sensing parameter, peak position change, was observed for every chlorothalonil concentration. The peak position depends on the refractive index of the medium. Thus, it is more reliable than intensity. The low absorption rate of $\Delta \lambda$ max occurs at 1.0 mM, whereas the high absorption of $\Delta \lambda$ max was obtained at 40.0 mM of the chlorothalonil concentration.

Figure 8 illustrates the transverse and longitudinal plasmonic resonance bands observed at varying concentrations of chlorothalonil. In the case of t-SPR, the resonance band remained constant in its wavelength position between 1.0 mM and 10.0 mM chlorothalonil, as the associated refractive index change was minimal, however, from 15.0 mM to 40.0 mM, a noticeable red shift in the t-SPR band occurred, attributed to the increasing refractive index of the surrounding medium. A similar red shift was observed in the l-SPR band, which progressively shifted from 1.0 mM up to 40.0 mM chlorothalonil, indicating its greater responsiveness to external environment changes than the t-SPR band.

This heightened sensitivity of the l-SPR can be explained by the tendency of gold nanoparticles to exhibit stronger longitudinal polarization. This enhanced polarization reduces the build-up of surface charge, thereby influencing the resonance frequency. As the refractive index increases, the resonance frequency decreases, resulting in a shift

toward longer wavelengths [24]. The corresponding data for these observations are summarized in Table 2. As previously discussed, variations in plasmonic behavior are

closely linked to the refractive index of the surrounding environment. Table 2 presents the chlorothalonil concentrations along with their respective index values.

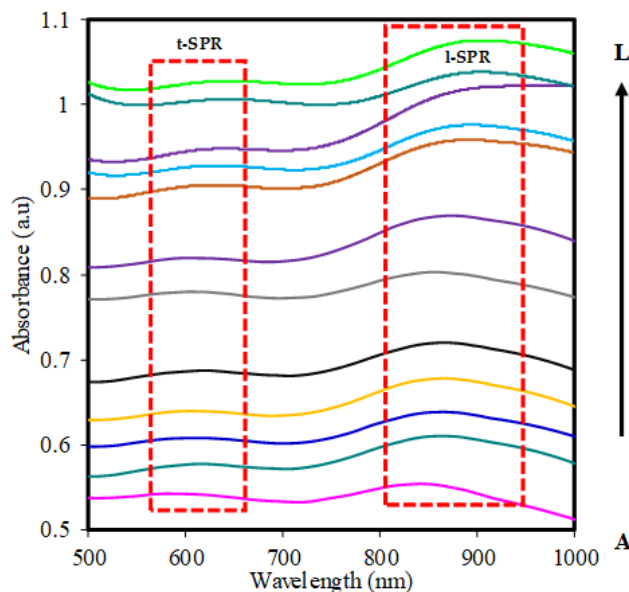


Figure 8. Absorbance spectra for t-SPR and l-SPR responses of AuNPs to varying chlorothalonil concentrations ranging from 1.0 mM to 40.0 mM. The concentrations are labeled as follows: A – 1.0 mM, B – 2.0 mM, C – 3.0 mM, D – 4.0 mM, E – 5.0 mM, F – 10.0 mM, G – 15.0 mM, H – 20.0 mM, I – 25.0 mM, J – 30.0 mM, K – 35.0 mM, and L – 40.0 mM.

Table 2 The t-SPR and l-SPR band peaks position of AuNPs with different chlorothalonil concentrations

Concentration of chlorothalonil (mM)	Intensity (I max)		Wavelength (λ max)		Index Bias (η)
	t-SPR	l-SPR	t-SPR	l-SPR	
1.0	0.542	0.554	599.82	848.61	1.3410
2.0	0.577	0.610	614.97	862.24	1.3490
3.0	0.607	0.638	613.96	862.27	1.3580
4.0	0.641	0.677	611.44	864.26	1.3648
5.0	0.687	0.721	609.92	864.76	1.3717
10.0	0.780	0.803	608.41	866.78	1.4014
15.0	0.820	0.868	606.90	868.80	1.4251
20.0	0.904	0.960	605.89	870.82	1.4443
25.0	0.929	0.977	603.87	873.84	1.4605
30.0	0.948	1.020	601.35	875.36	1.4740
35.0	1.006	1.041	598.82	879.90	1.4857
40.0	1.028	1.076	594.77	884.95	1.4956

The results in Table 2 indicate a consistent trend in peak shifts corresponding to increasing chlorothalonil concentrations, validating the sensitivity of the plasmonic sensor. The t-SPR and l-SPR bands red-shift with increasing chlorothalonil concentration. At 1.0 mM, the t-SPR peak is at 599.82 nm, shifting to 594.77 nm at 40.0 mM. The l-SPR peak follows a similar trend, shifting from 848.61 nm at 1.0 mM to 884.95 nm at 40.0 mM. The corresponding refractive index bias increases from 1.3410 to 1.4956, confirming the sensor's responsiveness to chlorothalonil concentration changes. Meanwhile, the absorbance intensity increases proportionally with chlorothalonil concentration, with t-SPR absorbance rising from 0.542 to 1.028 and l-SPR

absorbance increasing from 0.554 to 1.076. This trend suggests enhanced plasmonic interactions due to increased molecular adsorption at the nanoparticle surface. The observed red shifts in both resonance bands are consistent with prior research on LSPR sensors utilizing anisotropic gold nanoparticles. Comparable spectral shifts in SPR bands due to analyte concentration changes have been reported in studies on plasmonic sensors utilizing gold nanostructures [25]. The increase in absorbance intensity with analyte concentration also aligns with findings from previous plasmonic sensor studies, indicating effective chlorothalonil molecules' adsorption to the AuNPs surface.

4. CONCLUSION

This work demonstrates the sensitive detection of chlorothalonil by exploiting the surface plasmonic resonance of AuNPs. Bare AuNPs in the air were found to show two peaks representing the t-SPR and l-SPR response bands. The same results were obtained for AuNPs in DI water and chlorothalonil at different peak intensities and positions. 30.0 mM chlorothalonil without AuNPs shows almost consistent intensity with no significant peaks of both t-SPR and l-SPR. The sensing sensitivity of AuNPs-based LPSR sensor for chlorothalonil detection was analyzed using four sensing parameters, i.e., peak position and absorbance intensity for both t-SPR and l-SPR.

The chlorothalonil solution was diluted with 5 mL deionized water for twelve different concentrations, and results showed that a low absorption rate of $\Delta\lambda$ max occurred at 1.0 mM, whereas high absorption of $\Delta\lambda$ max was obtained at 40.0 mM of the chlorothalonil concentration. Besides, the stability of AuNPs had been tested for 10 minutes (600 seconds). Moreover, the t-SPR and l-SPR peaks showed a linear trend in concentration. Then, a repeatability test was done to validate the repeatability potential of a plasmonic sensor for chlorothalonil detection. The response showed good repeatability during six test cycles, as proven by both DI water and chlorothalonil intensities, which almost completely recovered to their original intensity after every cycle of medium change. In conclusion, the plasmonic sensor-based AuNPs exhibited excellent stability and repeatability with a high sensitivity response towards chlorothalonil.

CONFLICT OF INTEREST

Marlia Morsin and Rahmat Sanudin currently serve as academicians at Universiti Tun Hussein Onn Malaysia. Nur Liyana Razali is a postgraduate student at Universiti Tun Hussein Onn Malaysia. Suratun Nafisah is a lecturer at Institut Teknologi Sumatra (ITERA).

FUNDING

This research work was supported by Universiti Tun Hussein Onn Malaysia, through Tier 1 (Vot Q893) and the Postgraduate Research Grant (GPPS) (Vot H690). This research was partially funded by the Ministry of Higher Education (MoHE) Malaysia through the Fundamental Research Grant Scheme (FRGS/1/2023/STG05/UTHM/02/3). The authors thank Microelectronics & Nanotechnology-Shamsuddin Research Centre (MiNT-SRC), Universiti Tun Hussein Onn Malaysia, for the related facilities.

ETHICAL APPROVAL

This original work has not been published or submitted simultaneously for publication elsewhere.

REFERENCES

- [1] X. Peng *et al.*, "Reactive oxygen species signaling is involved in melatonin-induced reduction of chlorothalonil residue in tomato leaves," *J. Hazard. Mater.*, vol. 443, no. PA, p. 130212, 2023, doi: 10.1016/j.jhazmat.2022.130212.
- [2] S. Senthil-Nathan, "A Review of Resistance Mechanisms of Synthetic Insecticides and Botanicals, Phytochemicals, and Essential Oils as Alternative Larvicidal Agents Against Mosquitoes," *Front. Physiol.*, vol. 10, no. February, pp. 1–21, 2020, doi: 10.3389/fphys.2019.01591.
- [3] J. Jiang, Y. Yang, L. Wang, S. Cao, T. Long, and R. Liu, "Effects of Chlorothalonil Application on the Physio-Biochemical Properties and Microbial Community of a Yellow–Brown Loam Soil," *Agric.*, vol. 12, no. 5, 2022, doi: 10.3390/agriculture12050608.
- [4] Rupanshi *et al.*, *Biogenic Silver Nanoparticles as Next-Generation Green Catalysts for Multifaceted Applications*. Springer Nature Singapore, 2025. doi: 10.1007/s12209-025-00427-3.
- [5] T. Simões *et al.*, "From laboratory to the field: Validating molecular markers of effect in *Folsomia candida* exposed to a fungicide-based formulation," *Environ. Int.*, vol. 127, no. December 2018, pp. 522–530, 2019, doi: 10.1016/j.envint.2019.03.073.
- [6] M. E. Báez, B. Sarkar, A. Peña, J. Vidal, J. Espinoza, and E. Fuentes, "Effect of surfactants on the sorption-desorption, degradation, and transport of chlorothalonil and hydroxy-chlorothalonil in agricultural soils," *Environ. Pollut.*, vol. 327, no. December 2022, 2023, doi: 10.1016/j.envpol.2023.121545.
- [7] H. Tao, C. Fang, Y. Xiao, and Y. Jin, "The toxicity and health risk of chlorothalonil to non-target animals and humans: A systematic review," *Chemosphere*, vol. 358, no. August 2023, p. 142241, 2024, doi: 10.1016/j.chemosphere.2024.142241.
- [8] Y. Hua and G. Liu, *Food Pesticide Residues Monitoring and Health Risk Assessment*, vol. 13, no. 3. 2024. doi: 10.3390/foods13030474.
- [9] J. D. Maia, R. La Corte, J. Martinez, J. Ubbink, and A. S. Prata, "Improved activity of thyme essential oil (*Thymus vulgaris*) against *Aedes aegypti* larvae using a biodegradable controlled release system," *Ind. Crops Prod.*, vol. 136, no. May, pp. 110–120, 2019, doi: 10.1016/j.indcrop.2019.03.040.
- [10] G. P. Lim and M. S. Ahmad, "Development of Calcium alginate-chitosan microcapsules for encapsulation and controlled release of imidacloprid to control dengue outbreaks," *J. Ind. Eng. Chem.*, vol. 56, pp. 382–393, 2017, doi: 10.1016/j.jiec.2017.07.035.
- [11] S. Nafisah *et al.*, "Improved Sensitivity and Selectivity of Direct Localized Surface Plasmon Resonance Sensor Using Gold Nanobipyramids for Glyphosate Detection," *IEEE Sens. J.*, vol. 20, no. 5, pp. 2378–2389, 2020, doi: 10.1109/JSEN.2019.2953928.
- [12] G. N. P. Biosensors, "Gold Nanoparticle-Based Plasmonic Biosensors," 2023.

- [13] P. Borjikhani, N. Granpayeh, and M. I. Zibaii, "High sensitivity tapered fiber refractive index biosensor using hollow gold nanoparticles," *Sci. Rep.*, vol. 15, no. 1, p. 1458, 2025, doi: 10.1038/s41598-025-85739-z.
- [14] S. Nafisah, M. Morsin, R. Sanudin, N. L. Razali, Z. M. Zain, and M. Djamal, "Gold Nanobipyramids as LPSR Sensing Materials for Glyphosate Detection: Surface Density and Aspect Ratio Effect," *IEEE Sens. J.*, vol. 22, no. 19, 2022, doi: 10.1109/JSEN.2022.3199466.
- [15] A. Moslemi *et al.*, "Highly sensitive gold nanostar based optical fiber sensor with tunable plasmonic resonance," *Sensors and Actuators Reports*, vol. 9, no. April, p. 100326, 2025, doi: 10.1016/j.snr.2025.100326.
- [16] A. S. Côco, F. V. Campos, C. A. R. Díaz, M. C. C. Guimarães, A. R. Prado, and J. P. de Oliveira, "Localized Surface Plasmon Resonance-Based Nanosensor for Rapid Detection of Glyphosate in Food Samples," *Biosensors*, vol. 13, no. 5, 2023, doi: 10.3390/bios13050512.
- [17] E. V. R. Campos *et al.*, "Recent Developments in Nanotechnology for Detection and Control of Aedes aegypti-Borne Diseases," *Front. Bioeng. Biotechnol.*, vol. 8, no. February, pp. 1–17, 2020, doi: 10.3389/fbioe.2020.00102.
- [18] Y. Huang *et al.*, *Nanotechnology's frontier in combatting infectious and inflammatory diseases: prevention and treatment*, vol. 9, no. 1. 2024. doi: 10.1038/s41392-024-01745-z.
- [19] S. Nengsih, A. A. Umar, M. M. Salleh, and M. Oyama, "Detection of formaldehyde in water: A shape-effect on the plasmonic sensing properties of the gold nanoparticles," *Sensors (Switzerland)*, vol. 12, no. 8, pp. 10309–10325, 2012, doi: 10.3390/s120810309.
- [20] B. Nik and a El Sayed, "Preparation and Growth Mechanism of Gold Nanorods (NRs) Using Seed - Mediated Growth Method," *Chem. Mater.*, vol. 15, no. 16, pp. 1957–1962, 2003, doi: Doi 10.1021/Cm020732l.
- [21] M. Morsin, M. M. Salleh, M. Z. Sahdan, and F. Mahmud, "Effect of Seeding Time on the Formation of Gold Nanoplates," *Int. J. Integr. Eng.*, vol. 9, no. 2, pp. 27–30, 2017.
- [22] C. Kan *et al.*, "Synthesis of high-yield gold nanoplates: Fast growth assistant with binary surfactants," *J. Nanomater.*, vol. 2010, 2010, doi: 10.1155/2010/969030.
- [23] B. S, B. S, and G. S, "Plasmonic Sensors for Disease Detection - A Review," *J. Nanomed. Nanotechnol.*, vol. 7, no. 3, pp. 1–10, 2016, doi: 10.4172/2157-7439.1000373.
- [24] P. G. Martínez-torres, M. M. Martínez-garcía, P. E. Cardoso-ávila, and J. L. Pichardo-molina, "Facile Nanostructured Substrate Preparation Using Gold Nanocuboids for SERS Regular Paper," pp. 2–8, 2015, doi: 10.5772/60500.
- [25] P. Suvarnaphaet and S. Pechprasarn, "Enhancement of long-range surface plasmon excitation, dynamic range and figure of merit using a dielectric resonant cavity," *Sensors (Switzerland)*, vol. 18, no. 9, 2018, doi: 10.3390/s18092757.